Exploring approximations to the GW self-energy ionic gradients

C. Faber[1,2,3], P. Boulanger[1,2], C. Attaccalite[1,2], E. Cannuccia[4,5], I. Duchemin[2,3], T. Deutsch[2,3], X. Blase[1,2]
[1] *CNRS, Institut Néel, 38042 Grenoble, France,*
[2] *Université Grenoble Alpes, 38042 Grenoble, France,*
[3] *INAC, SP2M/L_sim, CEA cedex 09, 38054 Grenoble, France.*
[4] *Institut Laue Langevin, BP 156, 38042 Grenoble, France,*
[5] *Laboratoire de Physique des Interactions Ioniques et Moléculaires, Aix-Marseille Université/CNRS, Campus de Saint Jérôme, 13397 Marseille, France.*
(Dated: March 12, 2015)

The accuracy of the many-body perturbation theory GW formalism to calculate electron-phonon coupling matrix elements has been recently demonstrated in the case of a few important systems. However, the related computational costs are high and thus represent strong limitations to its widespread application. In the present study, we explore two less demanding alternatives for the calculation of electron-phonon coupling matrix elements on the many-body perturbation theory level. Namely, we test the accuracy of the static Coulomb-hole plus screened-exchange (COHSEX) approximation and further of the constant screening approach, where variations of the screened Coulomb potential W upon small changes of the atomic positions along the vibrational eigenmodes are neglected. We find this latter approximation to be the most reliable, whereas the static COHSEX ansatz leads to substantial errors. Our conclusions are validated in a few paradigmatic cases: diamond, graphene and the C_{60} fullerene. These findings open the way for combining the present many-body perturbation approach with efficient linear-response theories.

PACS numbers: 71.15.Qe,71.38.-k

I. INTRODUCTION

Electron-phonon coupling (EPC) occupies a prominent role in various fields of condensed matter physics, including phonon-mediated superconductivity, photoemission band gap renormalization, current carriers inelastic scattering or the lifetime of hot electrons. Concerning the calculation of EPC matrix elements on the *ab initio* level, up to now, mainly density functional theory (DFT)[1] and its perturbative linear response extensions (DFPT)[2,3] have been applied, providing important information at the microscopic level.

Recently, several studies questioned the accuracy of the DFT-based EPC matrix elements when obtained with (semi)local functionals such as LDA or PBE.[4] By way of example, the electron-phonon coupling involving specific electronic and phonon modes in graphene[5,6] and graphite,[7] the value of the electron-phonon coupling potential to states at the Femi level in the electron-doped fullerene,[8,9] superconducting bismuthates and transition-metal chloronitrides,[10] or the renormalization of the photoemission band structure of pentacene[11] and diamond crystals,[12] were shown to be affected by a significant underestimation of the EPC matrix elements when calculated within DFT and (semi)local functionals.

As a cure to such problems, many-body perturbation theory (MBPT) techniques within the so-called GW approximation[13–18] showed a clear improvement when compared to available experimental data.[5,7,9–12] Unfortunately, the kind of theories that are available within DFT, and in particular the powerful DFPT formalism,[2,3] are not yet available within the framework of MBPT. Existing GW calculations of EPC matrix elements have been therefore based on the frozen-phonon approach, necessitating a stepwise displacement of the atoms along the phonon modes with an explicit evaluation of the electronic structure on the GW level for each step. This demanding approach cannot be reconciled with very large unit cells and is thus only feasible for zone-center or zone-boundary phonon modes. Going beyond the frozen-phonon approach, in order to access EPC matrix elements on the GW level for a large number of electron and phonon wave vectors, remains a considerable challenge to the *ab initio* community. Significant work is still needed to come up with a scheme that may allow to generalize the pioneering above-mentioned studies to a much larger set of systems.

In the present study, we explore the merits of the static coulomb-hole plus screened exchange (COHSEX)[14,15,19–27] approximation to the GW self-energy for the calculation of the electron-phonon coupling matrix elements in the isolated fullerene molecule, in diamond and in graphene. Our definitions of the relevant EPC matrix elements follow previous studies related to the superconducting transition in the fullerides,[8,9] the zero-point motion renormalization of the gap in diamond[12] and the gap opening through electron-phonon coupling in graphene,[5] respectively. For the same set of systems, we also explore the accuracy of the constant-screening approximation, namely the assumption that the screened Coulomb potential can be considered, to linear order, as a constant upon small changes of the atomic

positions. Whereas COHSEX leads to non-negligible discrepancies, this latter approximation will be shown to be robust and accurate. The present results offer important perspectives in making the GW formalism amenable to the study of condensed matter phenomena involving electron-phonon coupling.

II. METHODOLOGY

We briefly introduce the many-body perturbation theory Green's function formalism, providing a solid framework for the calculation of quasiparticle energies E. In such an approach, the one-body quasiparticle eigenvalue equation reads:

$$\left(\frac{-\nabla^2}{2} + V^{ion}(\mathbf{r})\right)\phi(\mathbf{r}) + V^H(\mathbf{r})\phi(\mathbf{r}) + \int d\mathbf{r}'\, \Sigma(\mathbf{r},\mathbf{r}';E)\phi(\mathbf{r}') = E\phi(\mathbf{r}),$$

where V^{ion} and V^H are the ionic and Hartree potential, respectively. The self-energy $\Sigma(\mathbf{r},\mathbf{r}';E)$ replaces the well-known exchange-correlation potential of density functional theory or the exchange operator in the Hartree-Fock formalism. In general, it is non-local, energy-dependent and non-Hermitian. Derived within Schwinger's functional derivative approach to perturbation theory,[13] the GW approximation to the self-energy leads to:

$$\Sigma^{GW}(\mathbf{r},\mathbf{r}';E) = \frac{i}{2\pi}\int d\omega e^{i\delta\omega} W(\mathbf{r},\mathbf{r}';\omega)G(\mathbf{r},\mathbf{r}';E+\omega),$$

where G and W are the time-ordered one-particle Green's function and the dynamically screened Coulomb potential, respectively, and $\delta = 0^+$ a small positive infinitesimal.

The Coulomb-hole plus screened-exchange (COHSEX) representation of the GW self-energy was originally introduced using a time representation of G, W and Σ.[14,20,21] We follow Hybertsen and Louie[15] by using the following spectral representations of G and W:

$$\begin{aligned} G(\mathbf{r},\mathbf{r}';E+\omega) &= \sum_n \frac{\phi_n(\mathbf{r})\phi_n^*(\mathbf{r}')}{E+\omega-\varepsilon_n - i\delta\mathrm{sgn}(\varepsilon_n-\mu)} \\ W(\mathbf{r},\mathbf{r}';\omega) &= v(\mathbf{r},\mathbf{r}') + \int_0^\infty d\omega' \frac{2\omega' B(\mathbf{r},\mathbf{r}';\omega')}{\omega^2-(\omega'-i\delta)^2}, \end{aligned}$$

where G has been written in terms of one-body eigenstates ϕ_n and eigenenergies ε_n, typically starting DFT Kohn-Sham or Hartree-Fock solutions, and W in terms of its spectral function B. These expressions allow to obtain the pole structure of both G and W. From the residue theorem, one then rapidly obtains an *exact* decomposition of Σ:

$$\begin{aligned} \Sigma^{SEX}(\mathbf{r},\mathbf{r}';E) &= -\sum_n^{occ} W(\mathbf{r},\mathbf{r}';E-\varepsilon_n)\phi_n(\mathbf{r})\phi_n^*(\mathbf{r}') \\ \Sigma^{COH}(\mathbf{r},\mathbf{r}';E) &= \sum_n \phi_n(\mathbf{r})\phi_n^*(\mathbf{r}')\mathcal{P}\int_0^\infty d\omega' \frac{B(r,r';\omega')}{E-\varepsilon_n-\omega'}, \end{aligned}$$

where $\mathcal{P}$ indicates the principal value. Σ^{SEX}, which involves a summation over the occupied states only, originates from the poles of G. It is called the screened exchange interaction in analogy to the bare exchange term that can be obtained by replacing W with the energy-independent bare Coulomb potential v. Σ^{COH} originates from the poles of W and represents the Coulomb-hole contribution, since it can be shown to be related to the interaction of an electron with its related adiabatically built correlation hole.

The static approximation to the exact COHSEX decomposition assumes that $(E-\varepsilon_n) \simeq 0$ for all (n), leading to simplified static screened exchange and Coulomb-hole expressions, namely:

$$\begin{aligned} \Sigma^{SEX}_{static}(\mathbf{r},\mathbf{r}';0) &= -\sum_n^{occ} W(\mathbf{r},\mathbf{r}';0)\phi_n(\mathbf{r})\phi_n^*(\mathbf{r}') \\ \Sigma^{COH}_{static}(\mathbf{r},\mathbf{r}';0) &= \frac{1}{2}\sum_n \phi_n(\mathbf{r})\phi_n^*(\mathbf{r}')\widetilde{W}(\mathbf{r},\mathbf{r}';0) \\ &= \frac{1}{2}\delta(\mathbf{r}-\mathbf{r}')\widetilde{W}(\mathbf{r},\mathbf{r}';0). \end{aligned}$$

Here, $\widetilde{W} = (W-v)$ is the difference between the screened and bare Coulomb potential. As a result, besides being a static approximation, this Coulomb-hole term is also local in space. Such a static COHSEX approximation (labeled COHSEX here below) was shown to yield too large gaps in the case of semiconductors.[15] By way of example, in the present case of the C_{60} molecule, the COHSEX gap is found to be 5.3 eV, i.e. 0.4 eV larger than the ∼4.9 eV experimental gap.[67] Nevertheless, this has to be compared to the starting 1.6 eV DFT-LDA Kohn-Sham gap which is dramatically too small.

While it cannot be claimed that the static COHSEX approach is a good approximation to absolute quasiparticle energies, we emphasize that we are interested in quasiparticle energy differences upon small (infinitesimal) atomic lattice motions. The main assumption on which we rely to calculate the electron-phonon coupling within the COHSEX approximation is that the *variations* of the dynamical contribution to the self-energy can be neglected. This can be *a priori* rationalized by emphasizing that dynamical interactions are driven by the plasmons dynamics, collective excitations less sensitive to small atomic displacements than single-particle excitation energies and wave functions. It remains, however, that besides the static approximation, the spatially local character of the static COH term is at odds with the nonlocality of the full GW self-energy.

In order to further justify the following results concerning the constant screening approach, namely the second approximation we explore in this study, it is instructive to consider the GW plus Bethe-Salpeter formalism.[28–30] The latter is a many-body perturbation theory approach concerned with describing the linear response of a system with respect to a time-dependent external perturbation and thus the Bethe-Salpeter equation (BSE) is the MBPT analogue to time-dependent DFT. At the heart of the GW/BSE approach lies the variation $(\partial GW/\partial\lambda)$, where the "perturbation" λ is the one-body Green's function G. The most common approximation that has been shown to be remarkably accurate[31–33] is to replace the GW self-energy by its static COHSEX approximation, and to consider further that $(\partial W/\partial\lambda) = 0$. It is such a simplified scheme we aim to explore in the present study, differing in the fact that the perturbation λ is now induced by a vibrational distortion of the system.

III. TECHNICAL DETAILS

The many-body GW and COHSEX calculations for the isolated C_{60} fullerene are performed using the FIESTA code, an implementation of the GW formalism within a Gaussian basis.[34–36] We start from DFT-LDA eigenstates calculated with the SIESTA package[37] and a triple-zeta plus polarization (TZP) basis[38] for the description of the valence orbitals combined with standard norm-conserving pseudopotentials.[39] We use the resolution of the identity technique (RI-SVS) with an even-tempered auxiliary basis set formed of four Gaussians per angular channel (up to d character) with exponents between 0.2 and 3.2 Bohr^{-2}. With such a basis, our G_0W_0@LDA ionization potential and HOMO-LUMO gap are found to be 7.33 eV and 4.39 eV (B3LYP geometry), respectively, starting from a 1.66 eV DFT-LDA gap. This is in close agreement with the 7.45 eV and 4.40 eV plane wave G_0W_0@LDA values of Ref. 40 (LDA geometry). The G_0W_0@LDA gap remains smaller than the $\sim$4.9 eV experimental value, an issue that will be addressed by the partially self-consistent scheme used in the present study, as discussed below.

Following Ref. 8, we use the relaxed structure and phonon eigenmodes generated within a DFT-B3LYP approach using a 6-311G(d) basis. This was shown to provide vibrational frequencies in excellent agreement with Raman measurements.[8,41] Concerning the calculation of the EPC matrix elements, our present study follows the approach described in Refs. 8,9, where the electron-phonon coupling strength associated with the (electron-doped) lowest unoccupied 3-fold degenerate t_{1u} molecular orbital (LUMO) has been explored within DFT and GW. The specific choice of the LUMO level is dictated by the physics of the phonon-mediated superconducting transition in the fullerides.[42,43] We adopt the standard definition of the effective electron-phonon coupling potential V^{ep} that enters e.g. the McMillan formula for the superconducting transition temperature through the dimensionless parameter $\lambda = N(E_F)V^{ep}$, where $N(E_F)$ is the density of states at the Fermi level. Namely, V^{ep} reads in the so-called molecular limit:[44,45]

$$V^{ep} = \frac{1}{9M}\sum_{\nu}\frac{1}{\omega_\nu^2}\sum_{m=1}^{3}\left|\frac{\partial\epsilon_m}{\partial\mathbf{u}^\nu}\right|^2. \qquad (1)$$

Here, M is the mass of the carbon ions, ω_ν is the frequency of the vibrational mode with index (ν) and $\mathbf{u}^\nu$ is the vibrational polarization vector. As already discussed before, the electronic states with energy (ϵ_m) are limited to the 3-fold degenerate LUMO level. From group theory analysis it follows that only the H_g and A_g vibrational modes can couple to these states. A schematic representation of the t_{1u} level splitting as a function of the deformation amplitude along a H_g mode is provided in Fig. 1(a). The EPC matrix elements are consequently related to the slopes $(\partial\epsilon_m/\partial\mathbf{u}^\nu)$, showing a strong dependence on the formalism adopted to calculate the energies ϵ_m. These energy derivatives are calculated within the frozen phonon approach, using a symmetric five points finite-difference formula.

Such an effective electron-phonon potential was calculated for C_{60} in Refs. 8,9, both within DFT using diverse (semi)local and hybrid exchange-correlation functionals and GW. While DFT-LDA values were shown to significantly underestimate the coupling energy, DFT calculations performed with global hybrids containing 20%-30% of exact exchange and the GW approach were found[8,9] to compare favorably to gas phase experimental data.[46,47] As a drawback of DFT calculations with hybrids, it was evidenced that the resulting V^{ep} potential would quickly increase with the amount of exact exchange, yielding the usual question of the proper choice of the functional parameters for a given system.

In the present study, we are concerned with exploring simplified GW schemes, i.e approximations reducing the needed computational effort. As such, quasiparticle energies are evaluated at a single-shot COHSEX and a partially self-consistent evCOHSEX level, where the quasiparticle energies are reinjected self-consistently in the construction of G and W, while keeping the starting Kohn-Sham LDA wave functions unchanged. Our reference point are partially self-consistent evGW calculations with self-consistency on the eigenvalues as presented in Ref. 9 for the calculation of the EPC matrix elements in C_{60}. Such a simplified approach to full self-consistency, justified by the dramatically too small starting point DFT-LDA gap for small isolated molecules, has been shown in the case of gas phase organic systems to produce more accurate ionization potentials and electronic affinities,[34,35,48–51] together with improved optical excitation energies at the GW/BSE level,[36,52–54] when LDA or PBE Kohn-Sham eigenstates are chosen as starting points. Consistently, when starting from DFT-LDA, EPC matrix elements in C_{60} were also found to be in

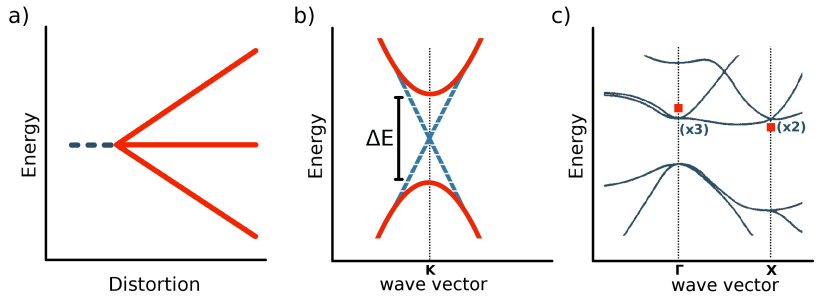

FIG. 1: Schematic representation of changes in the electronic structure under phonon distortion: a) in C_{60}, the 3-fold LUMO levels (blue) split under a distortion (red) along a H_g phonon mode. b) In graphene, an energy gap ΔE at the Dirac point is opened (red) when distorting the equilibrium structure (blue) along the $\Gamma - A_1'$ or $K - E_{2g}$ phonon modes. c) In diamond, the lowest lying conduction bands at Γ/X (blue) are renormalised by their coupling to a zone-boundary phonon mode. For clarity, only the states showing the largest shift are plotted (red dot, see text).

closer agreement with experiment within evGW as compared to G_0W_0.[9]

For the periodic diamond and graphene systems, we use the Yambo code which implements many-body perturbation theory within a plane wave formalism.[55] The starting DFT Kohn-Sham eigenstates are generated with the Abinit code.[56] In the case of graphene, the running parameters are identical to those used in a previous GW study of the electron-phonon coupling in this material,[5] namely we use $a = 2.46$ Å as lattice parameter, 15 a.u. distance between the layers,[57] $36 \times 36 \times 1$ **k**-points for the GW calculations in the Brillouin zone (BZ) corresponding to the primitive (2-atoms) cell and the nearest equivalent **k**-grid in the BZ corresponding to the supercell needed to describe zone-boundary ($\mathbf{q} = \mathbf{K}$) phonons in the frozen-phonon approach. The energy cutoff on the plane wave basis was set to 60 Ry. All conduction bands within an energy range of 45 eV above the Fermi level were used to build G and W, and a cutoff of 4 Ha for the construction of the dielectric function. The Godby-Needs plasmon pole model was employed for the dynamical dielectric constant entering in W.

As schematically described in Fig. 1(b), we focus on the splitting ΔE of the degenerate occupied and unoccupied levels at the Dirac point caused by the coupling to the $\mathbf{q}\nu = \mathbf{\Gamma}$-$E_{2g}$ optical mode at zone center together with the zone-boundary $\mathbf{q}\nu = \mathbf{K}$-$A_1^{'}$ phonon, for which the strongest renormalization of the coupling constant have been observed upon replacing the DFT-LDA approach by the G_0W_0 formalism.[5,6] The EPC matrix elements of interest are thus here related to the derivatives: $(\partial \Delta E/\partial \mathbf{u}_{\mathbf{q}\nu})$, namely (see Ref. 5):

$$\langle D^2_{\mathbf{q}\nu} \rangle = \frac{1}{A_{\mathbf{q}\nu}} \left(\frac{\partial \Delta E}{\partial \mathbf{u}_{\nu\mathbf{q}}} \right)^2, \qquad (2)$$

expressed in $(eV/\mathring{A})^2$, where $A_{\mathbf{q}\nu}$ equals 16 and 8 for $\mathbf{q}\nu = \mathbf{\Gamma}$-$E_{2g}$ and $\mathbf{q}\nu = \mathbf{K}$-$A_1^{'}$, respectively. We performed "single-shot" G_0W_0 and COHSEX calculations on top of DFT-LDA results, namely the standard perturbative (non self-consistent) GW approach to obtain quasiparticle energies.

For diamond, following Antonius and coworkers,[12] we have used a relaxed DFT-LDA geometry (lattice parameter $a = 3.591$ $\mathring{A}$) with a plane wave cutoff energy of 80 Ry and norm-conserving pseudopotentials. All calculations were performed with a 8x4x4 uniform Monkhorst-Pack grid to describe the supercell necessary for the frozen-phonon simulation of the ($\mathbf{q} = X$) phonon. We have used 160 bands and a cutoff of 8 Ha for the construction of the dielectric function and the GW self-energy. Following Refs. 12 and 58 where the diamond band-gap renormalization by the zero-point motion was studied, we define the relevant EPC matrix elements as the second derivative of the electronic eigenvalues with respect to the phonon displacements at equilibrium:

$$\frac{\partial \epsilon_{m\mathbf{k}}}{\partial n_{\nu\mathbf{q}}} = \frac{\hbar}{2M\omega_{\nu\mathbf{q}}} \frac{\partial^2}{\partial \mathbf{u}^2_{\nu\mathbf{q}}} \epsilon_{m\mathbf{k}}, \qquad (3)$$

where $n_{\nu\mathbf{q}}$ is the occupation of the phonon state (ν) of wave vector $\mathbf{q}$. The EPC matrix elements are now related to the temperature dependent renormalization of the electronic bands. We evaluate the second-derivative of the eigenvalues using a symmetric five-point finite-difference formula with displacements of 0.01, 0.02 and 0.03 Å. In Ref. 59, it was already shown that standard DFT and DFPT methods with (semi)local functionals strongly underestimate (by ca. 30%) the zero-point renormalization of the direct gap of diamond compared to experiment, while Ref. 12 demonstrated that G_0W_0 calculations restored the good agreement between theory and experiment. We focus here below on the renormalization of the lowest conduction band edge at ($m\mathbf{k} = \mathbf{X}_{1c}$) and ($m\mathbf{k} = \mathbf{\Gamma}_{15c}$) by the coupling to the ($\nu\mathbf{q} = \mathbf{X_4}$) phonon modes at the zone-boundary (see Fig. 1c). It is for such a phonon wave vector that the EPC matrix elements were found to be large and that also the GW correction was shown to be the most significant.[12] Following Ref. 12, the provided EPC matrix elements are

	LDA	G_0W_0	$G_0W_0(W)$	COHSEX	COHSEX(W)
Graphene					
Γ-E_{2g}	44.3	68.1 (65.2)	72.0	81.5	83.2
K-$A_1^{'}$	88.6	201(187)	207	260	256
Diamond					
$\mathbf{\Gamma}_{15c}$	1.281	0.611	0.657	1.311	1.445
$\mathbf{X}_{1c}$	-2.009	-1.031	-1.066	-2.124	-2.273

TABLE I: Calculated EPC-related quantities (see text) for graphene and diamond. In the case of graphene, these correspond to the splitting of the degenerate highest valence and lowest conduction band at the Dirac point under the influence of a ($\mathbf{q}\nu = \mathbf{\Gamma}$-$E_{2g}$) and ($\mathbf{q}\nu = \mathbf{K}$-$A_1^{'}$) phonon mode and are expressed in $(eV/\AA)^2$. Number in parenthesis are obtained with a plasmon pole energy of 7 eV, close to the graphene π-plasmon energy, instead of the 27 eV originally used in Ref. 5 (see text). For diamond, these are the results of equation (3) for the $\mathbf{X}_{1c}$ and $\mathbf{\Gamma}_{15c}$ conduction states and for the $\mathbf{X}_4$ zone-boundary phonon mode only (values in eV). This corresponds to twice the zero-point renormalization arising from this given phonon mode (see Ref. 12).

averaged over the degenerate electronic manifold considered (namely the 3 degenerate levels at zone-center and the 2 degenerate levels at the $\mathbf{X}_{1c}$ zone boundary).

IV. RESULTS

A. Reference GW calculations

We first reproduce for validation and for reference the previously published GW calculations related to EPC matrix elements in graphene, diamond and C_{60}. Our results are compiled in Table I for diamond and graphene and in Table II for C_{60}, respectively. Our LDA and G_0W_0 values for graphene are close to those found in Ref. 5, namely e.g. 201 eV/Å (G_0W_0 value, present study) for the largest matrix element with the ($\mathbf{K}$-$A_1^{'}$) phonon, to be compared to 193 eV/Å in the previous study.[57] The difference can be explained by an increased five points, instead of only two, finite-difference formula, and by the increase of the dielectric matrix size energy cutoff, from 2 to 4 Ha cutoff. We also verified that changing the Godby-Needs plasmon model input finite frequency, from the (default) 27 eV value in Ref. 5 to a 7 eV value closer to the π-plasmon resonance in graphene, does not change significantly the calculated EPC strength (see numbers in parenthesis in the Table I). Such differences are negligible with respect to the more than 100% increase as compared to the LDA value.

For diamond, the EPC contribution associated with the $m\mathbf{k} = \mathbf{\Gamma}_{15c}$ conduction states are in good agreement with the LDA and G_0W_0 results of Antonius and coworkers,[12] i.e. we find a 11 meV difference with respect to their EPC in the case of LDA, while we find a difference of 8 meV for the G_0W_0 results.[68] These small variations can be ascribed to the different pseudopotentials (Ref. 59 showed that pseudopotentials can lead to errors up to 50 meV), and to the different convergence parameters.

Since Ref. 12 focused on the renormalization of the direct band gap at the zone-center, comparison with the present results for the phonon coupling to the $\mathbf{X}_{1c}$ electronic state cannot be made. Our findings are, however, very consistent with what is observed for the $\mathbf{\Gamma}_{15c}$ state, namely a dramatic decrease of the coupling strength with the X_4 phonon mode which, again, is the dominant coupling mode. The coupling energy is indeed found to be reduced by 52% and 49% from LDA to GW for the $\mathbf{\Gamma}_{15c}$ and $\mathbf{X}_{1c}$ states, respectively. Since the $\mathbf{X}_{1c}$ state is closer to the true conduction band minimum, this is a strong indication that zero-point motion renormalization of the indirect gap will certainly also be strongly affected by the GW correction. The full study of such an effect is beyond the scope of the present paper.

For C_{60}, the total evGW coupling potential is within 8% of that found by Ref. 9 as a result of the larger TZP basis used here.[38] Our evGW V^{ep} potential is found to increase by 44% with respect to the corresponding LDA value, to be compared with the 48% increase obtained in Ref. 9 with a smaller basis. This indicates the good convergence of the GW correction to the LDA value. We note that while DFT and GW calculations are known to converge very differently with respect to basis size, we compare in the present study approaches which are much more similar, namely "standard and approximated" GW calculations, indicating certainly an even better convergence of the differences we are interested in.

B. The COHSEX approximation

We now explore approximations to the full GW calculations performed in Refs. 5,9,12 and reproduced here above. We start by the case of diamond. As compared to the G_0W_0 calculations, the static COHSEX approximation is shown to induce errors larger than 100% for the relevant electron-phonon coupling energy to the Γ_{15c} and X_{1c} states. In both cases, the static COHSEX approach strongly overestimates the electron-phonon coupling. A representation of the errors as compared to the G_0W_0 calculations is provided in Fig. 2.

The case of graphene is of specific interest since, in great contrast to diamond and C_{60}, the fundamental gap reduces to zero in the equilibrium geometry and opens

	Theory					Experiment
Mode	LDA	evGW	COHSEX	evCOHSEX	evCOHSEX(W)	
Fullerene						
$H_g(1)$	4.7	5.85	4.99	6.3	6.3	
$H_g(2)$	9.3	10.1	9.99	10.3	11.9	
$H_g(3)$	8.8	12.95	11.96	13.7	15.3	
$H_g(4)$	4.2	5.5	4.9	5.4	5.7	
$H_g(5)$	3.98	4.9	4.5	5.3	5.5	
$H_g(6)$	1.8	1.99	2.05	2.2	2.4	
$H_g(7)$	15.8	25.4	23.3	27.9	26.5	
$H_g(8)$	13.1	18.3	17.1	19.8	19.5	
$A_g(1)$	1.2	1.9	1.85	1.8	1.2	
$A_g(2)$	7.2	13.98	13.2	15.4	12.2	
Total A_g	8.4	15.9	15.0	17.2	13.4	
Total H_g	61.7	84.96	78.8	90.9	93.1	96.2[b],96.5[c]
Total	70.2	100.9 (108.6[a])	93.8	108.1	106.6	106.8[b]

TABLE II: Mode-resolved V_ν^{ep} coupling potential associated with the 3-fold degenerate C_{60} LUMO and the corresponding V^{ep} totals (in meV). For group symmetry reasons, only the H_g and A_g vibrational modes couple to this electronic state.
[a] Ref. 9,
[b] Ref. 46, Table V,
[c] Ref. 47.

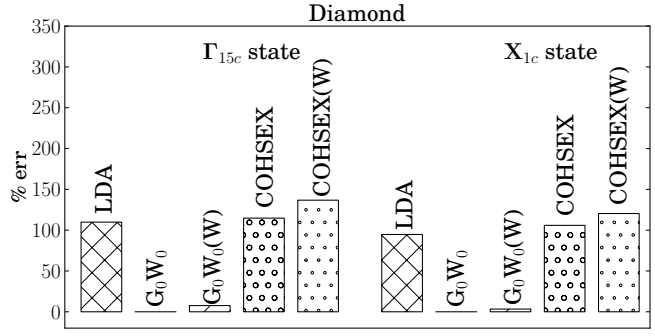

FIG. 2: Relative error of the different approximations with respect to the G_0W_0 results for the "thermal renormalization" EPC energies (Eqn. 3) for the lowest conduction band of diamond.

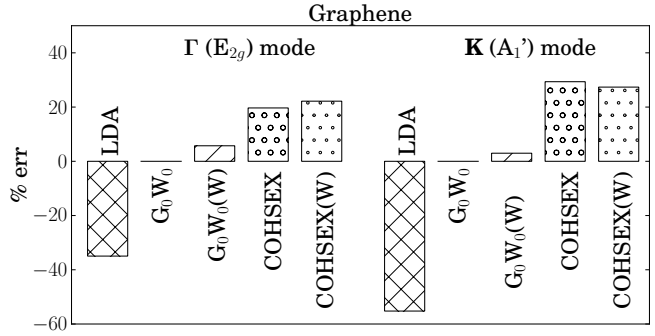

FIG. 3: Relative error of the different approximations with respect to the G_0W_0 results for the electron-phonon coupling in graphene.

upon phonon distortions. For the optical phonon mode at the zone-center, the COHSEX approximation leads again to an increase as compared to the G_0W_0 value, even though smaller than in the diamond case with a 20% error. Such an error becomes larger for the **K**-$A_1^{'}$ mode with a 29% increase of the EPC-related gap-opening rate. In the present graphene case, the error induced by the COHSEX approach remains smaller than the 34% and 56% reduction observed upon using DFT-LDA instead of G_0W_0. However, the close to 30% error observed for the COHSEX calculation of $\langle D^2_{\mathbf{K}} \rangle$ is clearly significant (see Fig. 3), questioning again the applicability of the static COHSEX formalism for EPC matrix elements calculations.

We now consider the C_{60} case, where we compare evGW and evCOHSEX calculations. A global increase of about 7% from evGW to its static approximation is observed. Besides the $H_g(4)$ and $A_g(1)$ modes showing very small couplings, the static COHSEX approximation is observed again to systematically increase the coupling strength as compared to evGW.[62] This result is consistent with what was observed for diamond and graphene, even though clearly the error appears to vary from one system to another.

C. The constant screening approximation

Following the above-mentioned analogy with the Bethe-Salpeter formalism, we finally test another approximation, that is the constant screening approach. Namely, we explicitly calculate the screened Coulomb potential for the undistorted structure and upon changing the positions of the ions along the ($\mathbf{R}_{\mathbf{q}\nu}$) vibrational eigenmodes, we keep W frozen to the undistorted value. Formally, this amounts to assuming that: $\partial GW/\partial \mathbf{u}^{\mathbf{q}\nu} \approx (\partial G/\partial \mathbf{u}^{\mathbf{q}\nu})W$. Such an approach will be labeled $GW(W)$ or $COHSEX(W)$ in the following.

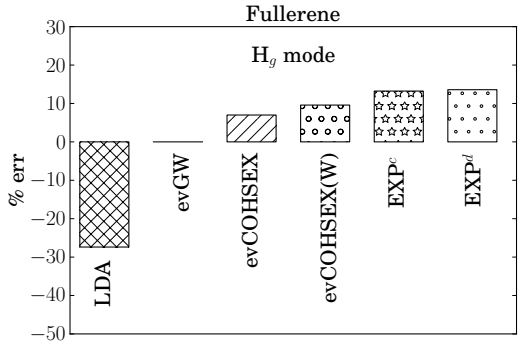

FIG. 4: Relative error of the different approximations with respect to the evGW results for the H_g-related V^{ep} of equation (1). For convenience, a comparison to the experimental data is provided.

In the case of the fullerene, where calculations are performed within a Gaussian basis, special care must be taken in the implementation of such a constant-screening approximation. In the auxiliary basis, or resolution of the identity approach, the bare and screened Coulomb potentials are expressed in terms of an atom-centered auxiliary basis with the following relations:

$$[W]_{\beta,\beta'} = \int\int d\mathbf{r}d\mathbf{r}'\beta(\mathbf{r})W(\mathbf{r},\mathbf{r}')\beta'(\mathbf{r}'), \qquad (4)$$

$$W(\mathbf{r},\mathbf{r}') = \sum_{\beta,\beta'} \beta(\mathbf{r}) \left(S^{-1}[W]S^{-1}\right)_{\beta,\beta'} \beta'(\mathbf{r}'), \qquad (5)$$

where S is the overlap matrix in the auxiliary basis. Using now the notation: $\underline{W}$ and $\underline{\beta}$ for the screened Coulomb potential and the auxiliary basis for the slightly distorted system, the assumption: $\underline{W}(\mathbf{r},\mathbf{r}') \simeq W(\mathbf{r},\mathbf{r}')$ leads straightforwardly to the condition:

$$[\underline{W}]_{\underline{\beta},\underline{\beta}'} \simeq S_{\underline{\beta}\beta}[W]_{\beta,\beta'}S_{\beta'\underline{\beta}'}, \qquad (6)$$

where $S_{\underline{\beta}\beta} =< \underline{\beta}|\beta >$ is an overlap matrix between the auxiliary bases for the perturbed and unperturbed systems, respectively.

For C_{60} again, we test the constant screening approximation at the COHSEX level only, namely comparing evCOHSEX and evCOHSEX(W) calculations of the V^{ep} energies. While the plasmon-pole approach used for diamond and graphene is based on a fixed finite frequency pole value independent of the geometry, the real axis poles contribution to the correlation energy in the contour deformation approach (see Refs. 19,34) implemented in the FIESTA package changes from one structure to another, leading to difficulties when trying to implement the constant-W approach within the frozen-phonon scheme.

The results of the constant-screening approximation are compiled in Tables I and II. For C_{60}, an excellent agreement is obtained within $evCOHSEX(W)$ compared to the corresponding evCOHSEX calculations. Comparing the total coupling, $evCOHSEX(W)$ and evCOHSEX agree within 1.5 %.

We now explore the constant-screening approximation for periodic diamond. Results are again compiled in Table I. For diamond, we observe a 3.4% and 7.5% difference between $G_0W_0(W)$ and G_0W_0 for the X_{1c} and Γ_{15c} states, respectively. At the COHSEX level, the constant screening approximation yields errors of the order of 7.0% and 10.2%, respectively. In summary, while the COHSEX approximation was failing for diamond, the constant-W approximation leads again to very reasonnable results, with errors well within 10% at the GW level. As illustrated in Fig. 2, this error is much smaller than the error induced by the LDA approximation.

We finally address the case of graphene. Concerning the coupling with the zone-center optical mode, the constant-W approach leads to a 5.7% and 2.1% error respectively when comparing $G_0W_0(W)$ to G_0W_0 and COHSEX(W) to COHSEX. In the case of coupling with the zone-corner $\mathbf{K}$-$A_1^{'}$ phonon mode, the discrepancy is of 3% and 1.5% applying the constant-screening approximation to GW and COHSEX approaches, respectively. Notice that the results for the constant-screening of the $\mathbf{K}$-$A_1^{'}$ phonon are affected by a numerical error of about 4%, therefore the discrepancy could be slightly larger. Anyway this difference is much smaller than the error induced by the standard DFT-LDA calculations, but also much smaller than the error induced by the static COHSEX formalism as compared to the reference GW calculation.

V. DISCUSSION

Clearly, among the two approximations explored here above, the constant-screening stands as a much better approach than the static COHSEX for the calculation of electron-phonon coupling matrix elements within the GW formalism. Overall, the largest error induced by the static COHSEX approximation is larger than 100% in the diamond case, while it is reduced to 7% in the case of the constant-screening approximation to full GW calculations.

The static COHSEX approximation is known to always overestimate band gaps. As proposed in Ref. 8, a too large band gap should lead to an underscreening of the electron-phonon interaction and consequently to enhanced EPC matrix elements. This is consistent with the fact that, within Hartree-Fock or with increasing exact exchange in hybrid functionals, the EPC matrix elements are found to steeply increase. The Hartree-Fock $\langle D^2_{\mathbf{\Gamma}}\rangle$ and $\langle D^2_{\mathbf{K}}\rangle$ coupling constants in graphene were found to be about 5 and 30 times larger, respectively, as compared to their GW analog,[5] while in C_{60} increasing the percentage of exact exchange from 20% to 30% in hybrid functionals was found to enhance the V^{ep} energy by about 15%.[8] Such an interpretation matches the observation that in graphene and C_{60}, the COHSEX EPC

coupling constants are larger than their corresponding GW reference. In the case of diamond, where we are concerned with the second-order derivatives, the effect of assuming a static approximation may be more difficult to interpret.

An important observation further is that the Coulomb-hole term is a local potential in the static COHSEX approximation, washing out spatial local-field effects, a observation that may potentially allow to understand the failure of the COHSEX approximation to reproduce accurately the evolution of the band structure with phonon deformation. In any case, the large variations of the induced errors from diamond to graphene and C_{60} is still to be understood, and we will just stand here on the observation that the static COHSEX approximation cannot be trusted to improve on DFT-LDA calculations.

Concerning the neglect of the gradient of W with respect to the ionic positions, such an approximation was already tested by Ismail-Beigi and Louie in the context of excited state ionic forces within the Bethe-Salpeter formalism,[63] showing good agreement with explicit finite-difference "exact" BSE calculations for small CO and NH_3 molecules. It is commonly assumed that the GW/BSE approach is much more resistant to approximations on W as compared to the GW approach for (charged) excitations. This is due to cancellations of errors between the electron-electron and electron-hole interactions. Namely, any error introduced in W is expected to affect excitonic interactions and quasiparticle gaps in opposite ways. Clearly, the present GW study of the variations of a given quasiparticle energy with respect to ionic positions cannot benefit from such cancellation of errors. Still, the constant-screening approximation turns to be a reliable approach to save on computational cost.

An important consequence of the present findings is that once the screened Coulomb potential $W(\mathbf{r}, \mathbf{r}'; \omega)$ is built for the equilibrium geometry, the calculation of the variations of the quasiparticle energies with respect to the perturbation (λ) only requires the evaluation of the variations of the Green's function G with respect to the perturbation. This can be performed within standard DFPT techniques, at least in the case of non-self-consistent G_0W_0 calculations where the Green's function assumes an explicit form in function of the input DFT eigenstates. This may invite, for systems such as C_{60}, to use G_0W_0 calculations starting from DFT eigenstates obtained with hybrid functionals, which have been shown to be a better starting point for finite-size systems.[54,64–66]

VI. CONCLUSIONS

We have explored two approximations for calculating self-energy gradients of interest for electron-phonon coupling, namely the two simplifications commonly used in the GW/Bethe-Salpeter calculations, that is the static COHSEX and the constant screening approximations. We explored these approaches in the case of diamond, graphene and C_{60}. Our findings suggest that the COHSEX approximation cannot be trusted to improve on the DFT-LDA values as clearly illustrated in particular in the case of diamond. On the contrary, the constant screening hypothesis, namely assuming that W remains to first order constant with respect to small ionic displacements, seems to be reliable, with a discrepancy no larger than 10%, even in the difficult case of graphene where the phonon perturbation dramatically affects the Dirac cone and the (semi)metallic nature of the graphene sheet. Even though a deeper understanding of the origin of the specific difficulties uncountered by the static COHSEX approximation would allow to better rationalize the validity and limits of the tested approximations, the present results offer promising perspectives to carry on such many-body evaluations of the electron-phonon coupling gradients with much reduced computer cost on realistic systems, including the study of periodic systems with arbitrary wave vector perturbation. Further studies are however required on a larger set of systems and physical observables in order to better assess the interest, with respect to common DFT calculations, of using the GW approach, and its various approximations, for calculating self-energy gradients with respect to ionic positions.

Acknowledgments. P.B. warmly acknowledges G. Antonius for providing the diamond phonon eigenmodes used in this study and for guiding our comparison with Ref. 12. C. A. acknowledges Daniele Varsano for the correction of some bugs in the Yambo code. C.F. is indebted to the French CNRS and CEA for Ph.D funding. P.B. acknowledges a postdoctoral fellowship from the French National Research Agency under Contract No. ANR-2012-BS04 PANELS. Computing time has been provided by the "Curie" national GENCI-IDRIS supercomputing center under contract No. i2012096655 and a PRACE European project under contract No. 2012071258. X.B. acknowledges illuminating discussions with Steven G. Louie and G. Antonius.

[1] P. Hohenberg and W. Kohn, Phys. Rev. **136**, B864-B871 (1964).
[2] S. Baroni, S. de Gironcoli, A. Dal Corso, and P. Giannozzi, Rev. Mod. Phys. **73**, 515 (2001).
[3] X. Gonze and C. Lee, Phys. Rev. B **55**, 10355 (1997).
[4] J. P. Perdew, K. Burke and M. Ernzerhof, Phys. Rev. Lett. **77**, 3865-3868 (1996).
[5] M. Lazzeri, C. Attaccalite, L. Wirtz, and F. Mauri, Phys. Rev. B **78**, 081406 (2008).
[6] D. Basko and I. L. Aleiner, Phys. Rev. B, **77**, 041409, (2008).
[7] A. Grüneis, J. Serrano, A. Bosak, M. Lazzeri, S. L. Molodtsov, L. Wirtz, C. Attaccalite, M. Krisch, A. Rubio, F. Mauri, and T. Pichler, Phys. Rev. B **80**, 085423

(2009).
[8] J. Laflamme Janssen, M. Côté, S.G. Louie, and M.L. Cohen, Phys. Rev. B **81**, 073106 (2010).
[9] C. Faber, J. Laflamme Janssen, M. Côté, E. Runge, and X. Blase Phys. Rev. B **84**, 155104 (2011).
[10] Z.P. Yin, A. Kutepov, and G. Kotliar, Phys. Rev. X **3**, 021011 (2013).
[11] S. Ciuchi, R. C. Hatch, H. Höchst, C. Faber, X. Blase, and S. Fratini, Phys. Rev. Lett. **108**, 256401 (2012).
[12] G. Antonius, S. Poncé, P. Boulanger, M. Côté, and X. Gonze, Phys. Rev. Lett. **112**, 215501 (2014).
[13] P.C. Martin and J. Schwinger, Phys. Rev. **115**, 1342 (1959).
[14] L. Hedin, Phys. Rev. **139**, A796 (1965).
[15] M.S. Hybertsen, S.G. Louie, Phys. Rev. B **34**, 5390 (1986).
[16] R.W. Godby, M. Schlüter, and L.J. Sham, Phys. Rev. B **37**, 10159 (1988).
[17] G. Onida, L. Reining, A. Rubio, Rev. Mod. Phys. **74**, 601 (2002).
[18] F. Aryasetiawan, O. Gunnarsson, Rep. Prog. Phys. **61**, 237 (1998).
[19] B. Farid, R. Daling, D. Lenstra, and W. van Haeringen, Phys. Rev. B **38**, 7530 (1988); B. Farid, in Electron Correlation in the Solid State, edited by N. H. March (World Scientific, Singapore, 1999), p. 217, and references therein.
[20] F. Bruneval, Ph.D. thesis, Ecole Polytechnique, Palaiseau, France, 2005.
[21] F. Bruneval, N. Vast, L. Reining, Phys. Rev. B **74**, 045102 (2006).
[22] M. Gatti, F. Bruneval, V. Olevano, L. Reining, Phys. Rev. Lett. **99**, 266402 (2007).
[23] F. Bruneval, N. Vast, L. Reining, M. Izquierdo, F. Sirotti, N. Barrett, Phys. Rev. Lett. **97**, 267601 (2006).
[24] F. Trani, J. Vidal, S. Botti, and M.A.L. Marques Phys. Rev. B **82**, 085115 (2010).
[25] J. Vidal, S. Botti, P. Olsson, J.-F. Guillemoles, and L. Reining, Phys. Rev. Lett. **104**, 056401 (2010).
[26] M.J. Lucero, I. Aguilera, C. Diaconu, P. Palacios, P. Wahnón, and G. E. Scuseria, Phys. Rev. B **83**, 205128 (2011).
[27] W. Kang, M.S. Hybertsen, Phys. Rev. B **82**, 195108 (2010).
[28] L.J. Sham and T.M. Rice, Phys. Rev. **144**, 708 (1966).
[29] W. Hanke and L.J. Sham, Phys. Rev. Lett. **43**, 387 (1979).
[30] G. Strinati, La Rivista del Nuovo Cimento **11** (12), 1-86 (1988).
[31] M. Rohlfing and S.G. Louie, Phys. Rev. Lett. **80**, 3320 (1998).
[32] L.X. Benedict, E.L. Shirley, and R.B. Bohn, Phys. Rev. Lett. **80**, 4514 (1998).
[33] S. Albrecht, L. Reining, R. Del Sole, G. Onida, Phys. Rev. Lett. **80**, 4510 (1998).
[34] X. Blase, C. Attaccalite, V. Olevano, Phys. Rev. B **83**, 536 115103 (2011).
[35] C. Faber, C. Attaccalite, V. Olevano, E. Runge, X. Blase, Phys. Rev. B **83**, 115123 (2011).
[36] X. Blase and C. Attaccalite, Appl. Phys. Lett. **99**, 171909 (2011).
[37] J.M. Soler, E. Artacho, J.D. Gale, A. García, J. Junquera, P. Ordejón, D. Sánchez-Portal, J. Phys.: Condens. Matter **14**, 2745 (2002).
[38] This triple-zeta plus polarization (TZP) basis consists of 3 shells of s and p orbitals, complemented by one polarization d shell, that is 19 orbitals per carbon atom, for the description of the eigenstates. This basis is larger than the double-zeta plus polarization (DZP) basis used in Ref. 9, with the inclusion in particular of diffuse s and p orbitals.
[39] N. Troullier and J.L. Martins, Phys. Rev. B **43**, 1993 (1991).
[40] T. Anh Pham, H.-V. Nguyen, D. Rocca, and G. Galli, Phys. Rev. B **87**, 155148 (2013).
[41] One has to note however that the impact of the functional on the vibrational eigenmodes used to calculate the EPC matrix elements was found to be marginal, the main effect coming from the framework within which the quasiparticle energies are calculated.
[42] A.F. Hebard *et al.*, Nature (London) *350*, 600 (1991).
[43] O. Gunnarsson, Rev. Mod. Phys. **69**, 575 (1997).
[44] V.P. Antropov, O. Gunnarsson, A.I. Liechtenstein, Phys. Rev. B **48**, 7651 (1993).
[45] Côté, M. and Grossman, J. C. and Cohen, M. L. and Louie, S. G., Phys. Rev. Lett. **81**, 697 (1998).
[46] N. Iwahara, T. Sato, K. Tanaka, and L.F. Chibotaru, Phys. Rev. B **82**, 245409 (2010). For an interpretation of the experimental data, see Note 21 of Ref. 9.
[47] I.D. Hands, J.L. Dunn, L. Janette, C.A. Bates, A. Colin, M.J. Hope, J. Michael, S.R. Meech, D.L. Andrews, Phys. Rev. B **77**, 115445 (2008). For an interpretation of the experimental data, see Note 22 of Ref. 9.
[48] P. H. Hahn, W. G. Schmidt, and F. Bechstedt, Phys. Rev. B **72**, 245425 (2005). In this study, the importance of correcting the starting eigenvalues in the construction of W is emphasized for molecular systems, bringing some light in the discussions concerning the update of the eigenvalues in the Green's function only (the GW_0 scheme) or in both G and W.
[49] L. Tiago, P. R. C. Kent, R. Q. Hood, and F. A. Reboredo, J. Chem. Phys. **129**, 084311 (2008).
[50] Sahar Sharifzadeh, Ariel Biller, Leeor Kronik, and Jeffrey B. Neaton, Phys. Rev. B **85**, 125307 (2012).
[51] Conor Hogan, Maurizia Palummo, Johannes Gierschner, and Angel Rubio, J. Chem. Phys. **138**, 024312 (2013).
[52] C. Faber, P. Boulanger, I. Duchemin, C. Attaccalite, and X. Blase, J. Chem. Phys. **139**, 194308 (2013).
[53] B. Baumeier, D. Andrienko, Y. Ma, and M. Rohlfing, J. Chem. Theory Comput. **8**, 997 (2012).
[54] P. Boulanger, D. Jacquemin, I. Duchemin, X. Blase, J. Chem. Theory Comput. **10**, 1212 (2014). The effect of partial self-consistency on the eigenvalues, with various starting-point wave functions, is discussed, in comparison with high-level coupled-cluster data.
[55] A. Marini, C. Hogan, M. Gruüning, and D. Varsano, Comput. Phys. Commun. **180**, 1392 (2009).
[56] X. Gonze et al., Comp. Mat. Science, **25**, 478 (2002).
[57] Notice that in Ref. 5 the interlayer distance between the graphene sheets is 15 a.u. and not 20 a.u. as it is wrongly reported in the paper.
[58] P. B. Allen and V. Heine, J. Phys. C **9**, 2305 (1976); P. B. Allen and M. Cardona, Phys. Rev. B **23**, 1495 (1981).
[59] S. Poncé, G. Antonius, P. Boulanger, et al; Comput. Mater. Sci. **83**, 341 (2014).
[60] For sake of indication, at the LDA level, the two lowest $\mathbf{X}_1$ and $\mathbf{X}_2$ vibrational modes lead to a (negative) -0.14 eV coupling energy, one order of magnitude smaller than the $\mathbf{X}_4$ mode coupling strength.
[61] P. Trevisanutto, C. Giorgetti, L. Reining, M. Ladisa and V. Olevano, Phys. Rev. Lett. **101**, 226405, (2008)
[62] We provide for information in Table II the results asso-

ciated with the (single-shot) COHSEX approach, starting from DFT-LDA eigenstates. Clearly, the EPC coupling energies approach from below the evGW value with an error not larger than that induced by the evCOHSEX technique. This stems from a cancellation of errors between the COHSEX approximation and the lack of self-consistency which leads to overscreening when building W directly from the DFT-LDA spectrum.

[63] S. Ismail-Beigi and S. G. Louie, Phys. Rev. Lett. **90**, 076401 (2003).

[64] Thomas Körzdörfer and Noa Marom, Phys. Rev. B **86**, 041110(R) (2012).

[65] F. Bruneval, M.A.L. Marques, J. Chem. Theory Comput. **9**, 324 (2013).

[66] S. Korbel, P. Boulanger, I. Duchemin, X. Blase, M.A.L. Marques, S. Botti, J. Chem. Theory Comput. **10**, 3934 (2014).

[67] The experimental band gap is taken from the NIST chemistry webbook at [http://webbook.nist.gov/chemistry/]. The band gap is calculated as the difference of the experimental ionization energy and electronic affinity. We adopt the most recent experimental data.

[68] Direct comparison with Figure 2 of Ref. 12 is not possible, since the figure presents the total electron-phonon coupling at wavevector $\mathbf{q} = \mathbf{X}$, i.e. all phonon modes are considered and not just X_4 as in this study. The comparison was made directly with the data used in Ref. 12 via personal correspondence.